Neutron scattering studies of spin excitations in superconducting $Rb_{0.82}Fe_{1.68}Se_2$

Miaoyin Wang,[1] Chunhong Li,[2] D. L. Abernathy,[3] Yu Song,[1] Scott V. Carr,[1] Xingye Lu,[1,2] Shiliang Li,[2] Zahra Yamani,[4] Jiangping Hu,[2,5] Tao Xiang,[2] and Pengcheng Dai[1,2,*]

[1]*Department of Physics and Astronomy, The University of Tennessee, Knoxville, Tennessee 37996-1200, USA*

[2]*Beijing National Laboratory for Condensed Matter Physics, Institute of Physics, Chinese Academy of Sciences, P.O. Box 603, Beijing 100190, China*

[3]*Quantum Condensed Matter Division, Oak Ridge National Laboratory, Oak Ridge, Tennessee 37831-6393, USA*

[4]*Canadian Neutron Beam Centre, National Research Council, Chalk River Laboratories, Chalk River, Ontario K0J 1J0, Canada*

[5]*Department of Physics, Purdue University, West Lafayette, Indiana 47907, USA*

(Received 16 January 2012; revised manuscript received 20 June 2012; published 5 July 2012)

We use inelastic neutron scattering to show that superconducting (SC) rubidium iron selenide $Rb_{0.82}Fe_{1.68}Se_2$ exhibits antiferromagnetic (AF) spin excitations near the in-plane wave vector $Q = (\pi,0)$ identical to that for iron arsenide superconductors. Moreover, we find that these excitations change from incommensurate to commensurate with increasing energy and occur at the expense of spin waves associated with the coexisting $\sqrt{5}\times\sqrt{5}$ block AF phase. Since these spin excitations cannot come from Fermi surface nesting based on angle resolved photoemission experiments, our results indicate the presence of local moments in SC $Rb_{0.82}Fe_{1.68}Se_2$ that may have a similar origin as the hourglass-like spin excitations in copper oxide superconductors.

DOI: 10.1103/PhysRevB.86.024502 PACS number(s): 74.25.Ha, 74.20.Rp, 74.70.Xa, 78.70.Nx

I. INTRODUCTION

All parent compounds of high-transition temperature (high-T_c) copper oxide superconductors are antiferromagnetic (AF) Mott insulators characterized by the same local moment Heisenberg Hamiltonian.[1,2] Although static long-range AF order in the parent compounds is suppressed upon electron or hole-doping to induce superconductivity,[1] short-range spin excitations persist in the doped materials and are believed to be associated with local moments important for the mechanism of superconductivity.[3] For iron-based superconductors,[4] the situation is more complicated. While superconductivity in iron pnictides also appears upon electron or hole-doping of their parent compounds,[4] the undoped materials are semimetals with Fermi surfaces composed of hole and electron pockets near $\Gamma(0,0)$ and $M(\pi,0)/M(0,\pi)$ points, respectively.[5] Since Fermi surface nesting between the hole and electron pockets can give spin-density wave order at wave vector $Q = (\pi,0)$,[5] the observation of such AF order in undoped materials[6] suggests that antiferromagnetism is due to Fermi surface nesting of itinerant electrons.[5] Moreover, inelastic neutron scattering experiments on single crystals of superconducting (SC) iron pnictides have found a resonance at $Q = (\pi,0)$ in the spin excitations spectra,[7–10] thus providing further evidence that superconductivity is due to sign reversed quasiparticle excitations between the hole and electron pockets.[11,12] Therefore, the microscopic origin of magnetism and superconductivity in iron pnictides appears to be fundamentally different from that of the copper oxides.[5]

In the case of alkaline iron selenide superconductors $A_yFe_{1.6+x}Se_2$ (A = K, Rb, Cs),[13–16] their parent compounds are insulators near $x = 0$[15,16] and form a $\sqrt{5}\times\sqrt{5}$ block AF structure with an Fe vacancy order [Fig. 1(a)][17–21] completely different from the collinear AF structure of the iron pnictides.[6] Furthermore, angle resolved photoemission (ARPES) experiments on SC $A_yFe_{1.6+x}Se_2$ revealed only electron Fermi surfaces at the $M(\pi,0)/M(0,\pi)$ points and no hole Fermi surface near $\Gamma(0,0)$.[22–24] Therefore, there is no Fermi surface nesting between $\Gamma(0,0)$ and $M(\pi,0)/M(0,\pi)$ points, which can give AF spin excitations at $Q = (\pi,0)$ [Fig. 1(c)].[25] Instead, the nesting properties between the $M(\pi,0)/M(0,\pi)$ electron pockets with d-wave symmetry can produce a broad plateau-like maximum around $Q = (\pi,\pi)$ that is bordered by two peaks at $Q \approx (\pi,0.625\pi)$ and $Q \approx (0.625\pi,\pi)$.[26] Although the recent discovery of the neutron spin resonance in SC $Rb_yFe_{1.6+x}Se_2$ at wave vector $Q = (\pm\pi,\pm0.5\pi)$ [or $Q = (\pm0.5\pi,\pm\pi)$] [Fig. 1(d)][27,28] is consistent with this picture,[26] it remains unknown whether there are also spin excitations near wave vectors $Q = (\pi,0)$ not associated with the Fermi surface nesting.

In this article, we use neutron scattering to map out the low-energy spin excitations in SC $Rb_{0.82}Fe_{1.68}Se_2$ [T_c = 32 K; Fig. 1(f)]. In addition to confirming the neutron spin resonance at $Q = (\pm\pi,\pm0.5\pi)$,[27,28] we find evidence for incommensurate spin excitations near wave vector $Q = (\pi,0)$ that are absent in insulating $Rb_{0.89}Fe_{1.58}Se_2$ [Figs. 1(b) and 1(d)].[29] With increasing energy, the incommensurate spin excitions disperse inward to $Q = (\pi,0)$ and disappear above E = 30 meV (Figs. 2 and 3). A comparison of spin excitations in the SC $Rb_{0.82}Fe_{1.68}Se_2$ with spin waves in the insulating $Rb_{0.89}Fe_{1.58}Se_2$[29] reveals that the intensity gain of the $Q = (\pi,0)$ excitations is at the expense of spin waves associated with the $\sqrt{5}\times\sqrt{5}$ AF phase (Figs. 4 and 5). Since electron-hole pocket excitations are impossible between $\Gamma(0,0)$ and $M(\pi,0)/M(0,\pi)$ points,[22–24] our results suggest the presence of local moments.[30] Moreover, the dispersion of the $Q = (\pi,0)$ excitations is similar to that of copper oxide superconductors[31,32] and insulating cobalt oxide,[33] thus suggesting the possible presence of dynamic stripes.[34]

II. EXPERIMENTAL RESULTS

We have performed inelastic neutron scattering experiments on the ARCS chopper spectrometer at the Spallation Neutron Source, Oak Ridge National Laboratory, using identical

 ©2012 American Physical Society

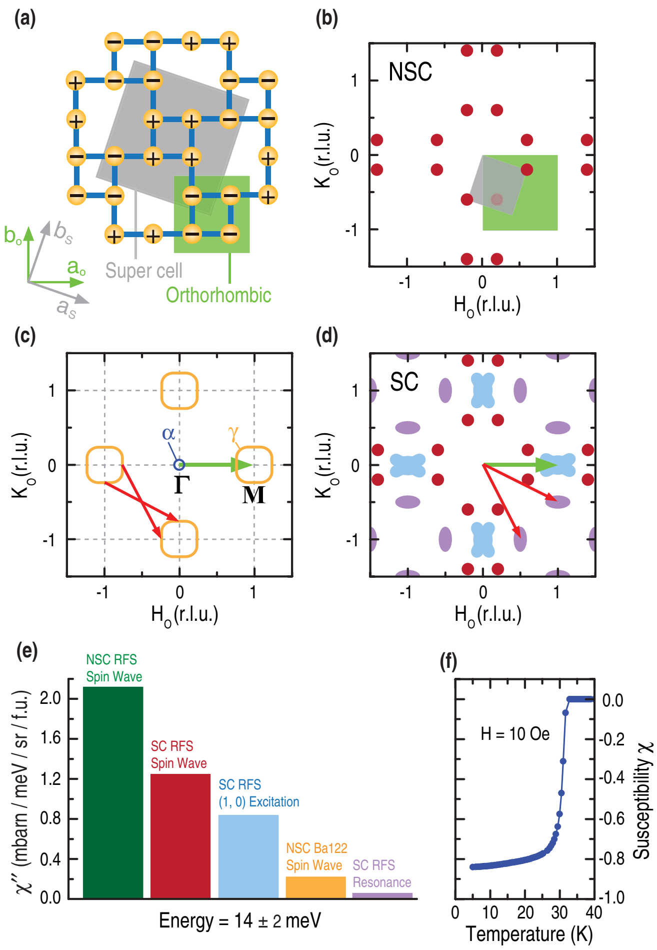

FIG. 1. (Color online) (a) The block AF order of the insulating $A_y\mathrm{Fe}_{1.6+x}\mathrm{Se}_2$, where the $\sqrt{5}\times\sqrt{5}$ superlattice structure is marked as gray with lattice parameter $a_s = 8.663$ Å and the orthorhombic lattice cell is shaded green.[29] (b) The reciprocal space in the $[H_o, K_o]$ plane, where the red circles indicate the AF Bragg peak positions. (c) Schematics of the Fermi surfaces of the SC $A_y\mathrm{Fe}_{1.6+x}\mathrm{Se}_2$. There are four large electron pockets at $Q = (\pm1,0)/(0,\pm1)$ and a small electron pocket at $\Gamma(0,0)$.[22–24] The neutron spin resonance should originate from the electron-electron pocket excitations.[27,28] The green arrow indicates the $\Gamma \leftrightarrow M$ transition. (d) Positions of observed spin excitations in the SC $\mathrm{Rb}_{0.82}\mathrm{Fe}_{1.68}\mathrm{Se}_2$, where spin waves from the block AF phase, neutron spin resonance, and $(\pi,0)$ excitations are marked as red solid circles, purple ellipses, and light-blue cross shapes, respectively. (e) Integrated intensity comparison of several samples at $E = 14 \pm 2$ meV. Olive green: spin waves in the insulating $\mathrm{Rb}_{0.89}\mathrm{Fe}_{1.58}\mathrm{Se}_2$; Dark red, light blue, and light violet are spin waves, $(\pi,0)$ excitations, and resonance in SC $\mathrm{Rb}_{0.82}\mathrm{Fe}_{1.68}\mathrm{Se}_2$; Orange: spin wave in $\mathrm{BaFe_2As_2}$. (f) Susceptibility measurement indicates $T_c = 32$ K.

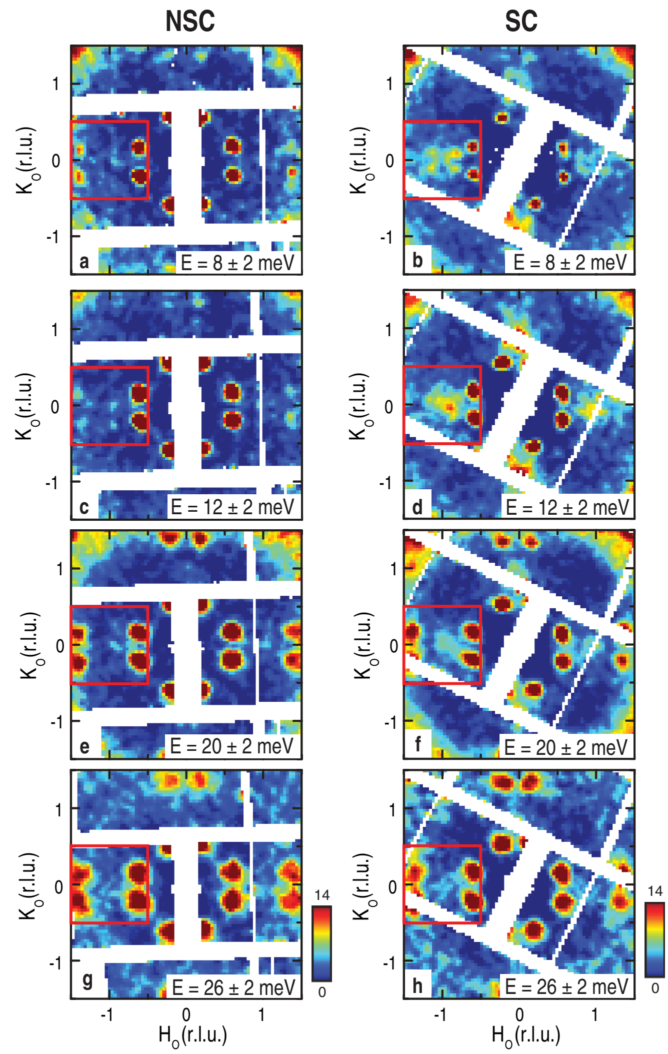

FIG. 2. (Color online) (a,c,e,g) Wave-vector dependence of spin-wave excitations at different energies for the NSC $\mathrm{Rb}_{0.89}\mathrm{Fe}_{1.58}\mathrm{Se}_2$ at 10 K obtained with incident neutron energy of $E_i = 80$ meV.[29] (b,d,f,h) Identical images for the SC $\mathrm{Rb}_{0.82}\mathrm{Fe}_{1.68}\mathrm{Se}_2$ at 6 K. The red squares are the Brillouin zone for iron pnictides.[35] The vertical color bars indicate intensity scale in mbarns/sr/meV/f.u.

conditions as previous work on spin waves in the insulating $\mathrm{Rb}_{0.89}\mathrm{Fe}_{1.58}\mathrm{Se}_2$.[29] Figures 1(a) and 1(b) show the block AF structure and the positions of the AF peaks in reciprocal space, respectively.[29] We define the wave vector Q at (q_x,q_y,q_z) as $(H_o,K_o,L_o) = (q_x a_o/2\pi, q_y a_o/2\pi, q_z c_o/2\pi)$ rlu, where $a_o = 5.48$ and $c_o = 14.69$ Å are the orthorhombic cell lattice parameters similar to iron pnictides.[35] In this notation, the neutron spin resonance[27,28] occurs at $Q = (\pm1,\pm0.5)$ [or $Q = (\pm\pi,\pm0.5\pi)$] [Fig. 1(d)], while the $\Gamma \leftrightarrow M$ Fermi surface nesting gives scattering at $Q = (\pm1,0)$ rlu [Figs. 1(c) and 1(d)]. We coaligned ~6 grams of SC single crystals $\mathrm{Rb}_{0.82}\mathrm{Fe}_{1.68}\mathrm{Se}_2$ grown by the self-flux method (with mosaic of ~6°),[29] where the chemical composition was determined by inductively coupled plasma analysis. Figure 1(f) shows the temperature dependence of the susceptibility measurements confirming $T_c = 32$ K. To ensure that the neutron spin resonance at $Q = (-1,0.5)$ and $E = 14$ meV[27,28] does not fall into the detector gaps on ARCS, we rotated the co-aligned samples counter-clockwise by ~27 degrees. The incident beam energies were $E_i = 35,80$ meV with E_i parallel to the c axis. The scattering was normalized to absolute units using a vanadium standard.[29]

From earlier work on $A_y\mathrm{Fe}_{1.6+x}\mathrm{Se}_2$,[18–21] we know that superconductivity coexists with the block AF order. Therefore, one should expect spin waves in SC $\mathrm{Rb}_{0.82}\mathrm{Fe}_{1.68}\mathrm{Se}_2$ from the block AF phase.[29] Figure 2 summarizes the two-dimensional constant-energy (E) images of spin excitations in the $[H_o, K_o]$

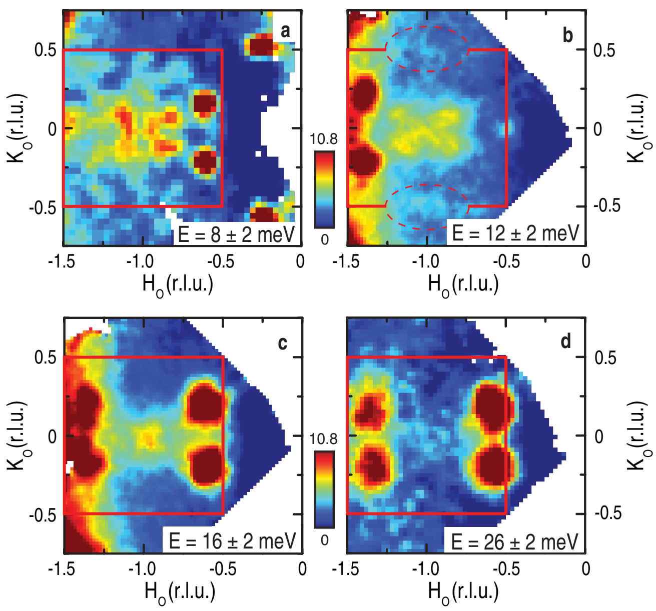

FIG. 3. (Color online) (a–d) Expanded view of the excitations near $Q = (1,0)$. The data in (b,c) are collected with $E_i = 35$ meV, while (a,d) are taken with $E_i = 80$ meV. The dashed ellipses in (b) mark positions of the resonance.

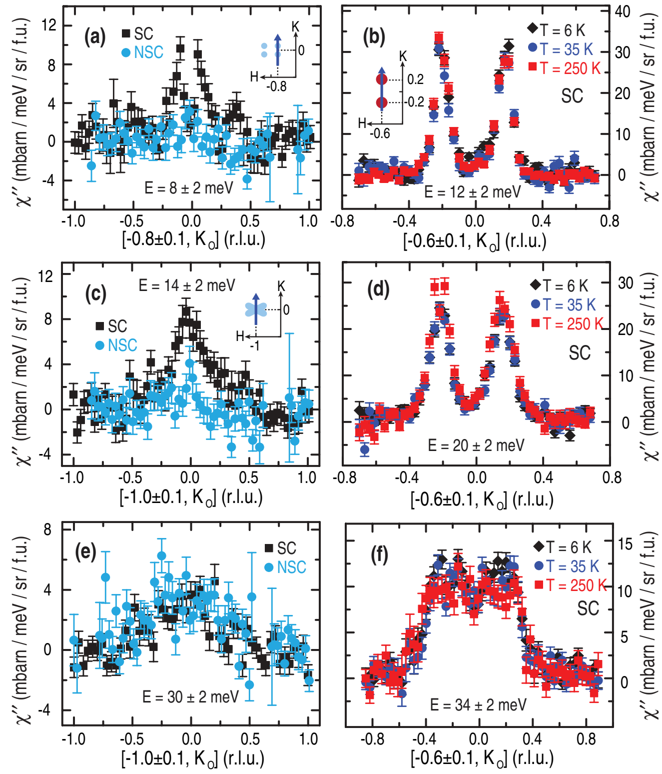

FIG. 4. (Color online) Constant energy cuts of data described in the legend of Fig. 2 converted into units of magnetic response $\chi''(Q,\omega)$ (after subtracting constant backgrounds and correcting for the Bose factor.) for the SC $Rb_{0.82}Fe_{1.68}Se_2$ and insulating $Rb_{0.89}Fe_{1.58}Se_2$. (a) Along the incommensurate positions at $E = 8 \pm 2$ meV, (c) along the commensurate positions at $E = 14 \pm 2$ meV, and (e) along the commensurate positions at $E = 30 \pm 2$ meV. Temperature dependence of $\chi''(Q,\omega)$ for spin waves from the $\sqrt{5} \times \sqrt{5}$ AF block phase at 6, 35, and 250 K with spin-wave energies of (b) $E = 12 \pm 2$, (d) 20 ± 2, and (f) 34 ± 2 meV.

plane for insulating and SC $Rb_yFe_{1.6+x}Se_2$. Since the subtle changes in the insulating and SC samples[18–21] are not expected to much affect phonons in these materials, we assume that the new dispersive features in $Rb_{0.82}Fe_{1.68}Se_2$ are spin excitations not associated with the insulating phase. Figures 2(a), 2(c), 2(e), and 2(g) show images of spin waves at energies $E = 8 \pm 2$, 12 ± 2, 20 ± 2, and 26 ± 2 meV, respectively, for the insulating $Rb_{0.89}Fe_{1.58}Se_2$.[29] They are centered at the expected AF wave vectors with no observable features at $Q = (1,\pm 0.5)$ and $Q = (1,0)$.[29]

Figures 2(b), 2(d), 2(f), and 2(h) plot images of the identical constant-energy cuts for the SC $Rb_{0.82}Fe_{1.68}Se_2$ at $T = 6$ K. In addition to the usual spin waves from the block AF structure, we find new features near $Q = (\pm 1,0)$ and $Q = (0,\pm 1)$. At $E = 8 \pm 2$ meV, there are four incommensurate peaks centered at $Q \approx (-1 \pm 0.14,\pm 0.1)$ [Fig. 2(b)]. Upon increasing energies to $E = 12 \pm 2$ [Fig. 2(d)] and 20 ± 2 meV [Fig. 2(f)], the excitations become approximately centered at $Q = (\pm 1,0)$. Finally, at $E = 26 \pm 2$ meV, they disappear at $Q = (\pm 1,0)$ and spin waves in the SC $Rb_{0.82}Fe_{1.68}Se_2$ and insulating $Rb_{0.89}Fe_{1.58}Se_2$ become indistinguishable [Figs. 2(g) and 2(h)]. Figures 3(a)–3(d) show the expanded view of the spin excitations near $Q = (-1,0)$ at different energies. At $E = 8 \pm 2$ meV, we see four distinct peaks [Fig. 3(a)]. At $E = 12 \pm 2$ meV, the excitations become cross-like near $Q = (-1,0)$ and one can also see the resonance centered at $Q = (-1,\pm 0.5)$[Fig. 3(b)].[27,28] For $E = 16 \pm 2$ meV, the excitations are well centered at $Q = (-1,0)$ [Fig. 3(c)]. Finally, at $E = 26 \pm 2$ meV, we find only spin waves from the block AF phase centered around the expected AF positions [Fig. 3(d)].

To directly compare excitations near the antiferromagnetic wave vector $Q = (-1,0)$ for the SC $Rb_{0.82}Fe_{1.68}Se_2$ and insulating $Rb_{0.89}Fe_{1.58}Se_2$, we carried out identical cuts for these two samples in absolute units. Figures 4(a) and 4(c) show comparisons at $E = 8 \pm 2$ and 14 ± 2 meV; there are clear excitations for the superconducting sample that are much weaker in the insulating sample. At $E = 30 \pm 2$ meV, there are no observable differences for these two samples. Figures 4(b), 4(d), and 4(f) show Bose population corrected $\chi''(Q,\omega)$ for spin waves from the $\sqrt{5} \times \sqrt{5}$ AF block phase at 6, 35, and 250 K. We find that spin waves from the block AF phase are temperature independent between 10 and 250 K.

To see how the excitations near $Q = (1,0)$ respond to superconductivity and determine whether they are related to spin waves from the block AF phase, we show in Fig. 5 constant-energy cuts for the $Q = (1,0)$ excitations and block AF spin waves at different temperatures. The neutron scattering cross section $S(Q,E)$ is related to the imaginary part of the dynamic susceptibility $\chi''(Q,\omega)$ by correcting for the Bose population factor via $S(Q,E) = 1/\{1 - \exp[-E/(k_BT)]\}\chi''(Q,E)$, where k_B is the Boltzmann's constant. Figures 5(a), 5(c), and 5(e) show constant-energy cuts along the K_o direction for different temperatures at $E = 8 \pm 2$, 12 ± 2, and 16 ± 2 meV, respectively. While $\chi''(Q,\omega)$ at the probed energies show no appreciable changes across T_c, it decreases on warming to $T = 250$ K, consistent with spin excitations. For comparison,

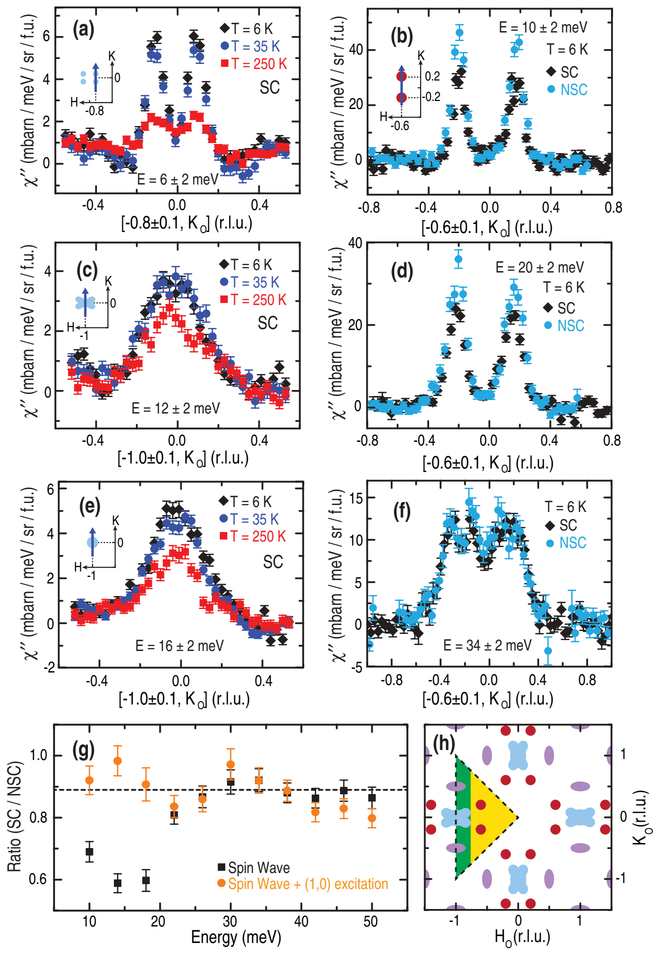

FIG. 5. (Color online) Cuts of $\chi''(Q,\omega)$ along (a) the $[-0.8 \pm 0.1, K]$, (c,e) $[-1 \pm 0.1, K]$ directions for the $Q = (-1,0)$ excitations at different temperatures. (b,d,f) Comparison of the low-temperature spin wave intensities for SC and insulating samples using the same cuts along the $[-0.6 \pm 0.1, K]$ direction. The spin wave intensity of the SC sample are lower at (b) $E = 12 \pm 2$ and (d) 20 ± 2 meV but become similar as that of the insulating sample at (f) $E = 34 \pm 2$ meV. (g) The black squares are the ratio of spin-wave intensity in the yellow area for SC and insulating samples. The orange circles are the ratio of excitations in (h) yellow area + green area for SC and insulating samples.

we find that $\chi''(Q,\omega)$ of the spin waves from the block AF phase are temperature independent between 10 and 250 K. This is expected since spin waves are bosons and should follow the Bose factor below T_N (Fig. 4). To see if superconductivity has any effect on spin waves of the block AF phase, we show in Figs. 5(b), 5(d), and 5(f) $\chi''(Q,\omega)$ for SC $Rb_{0.82}Fe_{1.68}Se_2$ and insulating $Rb_{0.89}Fe_{1.58}Se_2$. While the spin wave intensity at $E = 10 \pm 2$ and 20 ± 2 meV in the superconductor are lower than that of the insulator, it becomes similar at $E = 34 \pm 2$ meV. To quantitatively determine the differences between the intensity gain near $Q = (-1,0)$ with intensity loss of the AF spin waves in superconductor compared with that of the insulator, we plot in Fig. 5(g) the intensity ratio of SC and insulating samples (SC/NSC) as black squares [yellow area in Fig. 5(h)] and orange circles [yellow plus green areas in Fig. 5(h)], respectively. We see that the spin wave intensity

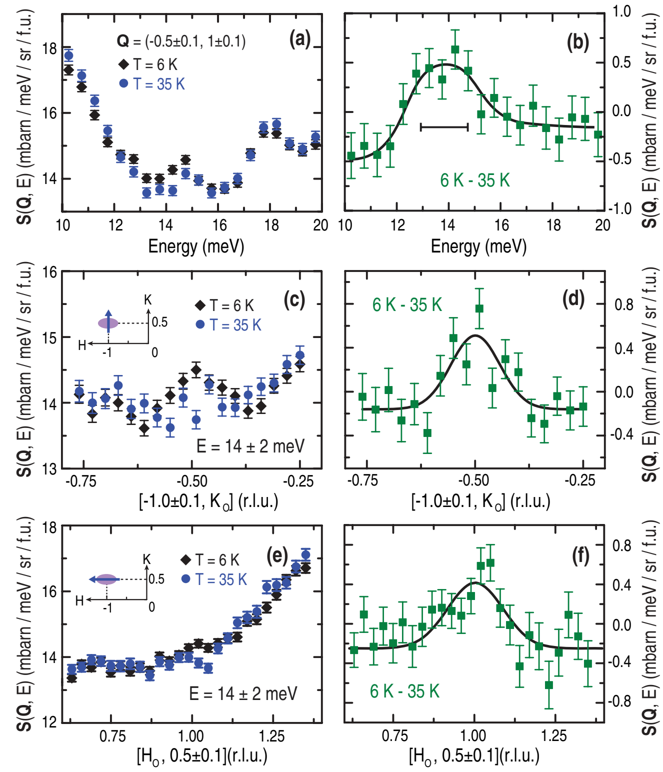

FIG. 6. (Color online) (a) Energy cut at the resonance position by integrating $Q = (-0.5 \pm 0.1, 1 \pm 0.1)$. (b) 6 K–35 K data shows a resonance at $E = 14$ meV with solid curve guides to the eye. The horizontal bar is the instrumental energy resolution. (c,e) Constant-energy cuts along the $[H, 1 \pm 0.1]$ and $[0.5 \pm 0.1, K]$ directions, respectively. (d,f) 6–35 K data confirm the resonance peak at $(1,-0.5)$ with a width $FWHM = 0.13 \pm 0.04$ along the H direction and $FWHM = 0.20 \pm 0.05$ along the K direction. The black curves are Gaussian fits to the peaks in (d,f).

loss below ~30 meV is approximately compensated by an intensity gain from excitations around $(-1,0)$.

Finally, to confirm the neutron spin resonance near $E = 14$ meV at $Q = (-1,0.5)$ in our SC $Rb_{0.82}Fe_{1.68}Se_2$,[27,28] we carried out constant-Q and constant-energy cuts to the data in Fig. 3(b) below and above T_c. Figure 6(a) shows the $S(Q,E)$ for integrated wave vectors $Q = (-0.5 \pm 0.1, 1 \pm 0.1)$ at 6 and 35 K. The temperature difference plot (6–35 K) in Fig. 6(b) has a clear peak at $E = 14$ meV, thus confirming the resonance below T_c.[27,28] Figures 6(c) and 6(e) show constant-energy cuts along the two different high symmetry directions (see insets) below and above T_c. The temperature difference plots show well-defined peaks at the expected wave vector.[27,28] Figure 1(e) compares the strength of the spin waves from the block AF structure in insulating and SC samples, the (1,0) spin excitations, the resonance, and spin waves of $BaFe_2As_2$[35] near $E = 14$ meV.

III. DISCUSSIONS AND CONCLUSIONS

The discovery of spin excitations near the $(\pi,0)$ wave vector and their dispersion in the SC $Rb_{0.82}Fe_{1.68}Se_2$ have several important implications. First, since ARPES experiments reveal that SC $A_yFe_{1.6+x}Se_2$ have no hole-like Fermi surface at

$\Gamma(0,0)$,[22–24] the $(\pi,0)$ spin excitations cannot arise from quasiparticle excitations between Γ and M points and most likely come from localized magnetic moments.[30] Taking into account that the SC $Rb_{0.82}Fe_{1.68}Se_2$ also has a neutron spin resonance most likely arising from Fermi surface nesting and itinerant electrons,[27,28] these results suggest that localized moments and itinerant electrons are both important ingredients for magnetism in alkaline iron selenide superconductors. Second, the observation of low-energy incommensurate spin excitations and its inverse dispersion are reminiscent of the spin excitations for copper oxide superconductors[31,32] and insulating $La_{2-x}Sr_xCoO_4$.[33] This suggests that the $(\pi,0)$ spin excitations stem from strongly correlated electronic physics and may be associated with dynamic stripes.[34] Third, the reduction in the low-energy spin wave intensity for the block AF phase in the SC $Rb_{0.82}Fe_{1.68}Se_2$ and the concurrent appearance of the incommensurate spin excitations near $Q = (\pi,0)$ indicate that spin excitations in superconductors are compensated by spin waves in the AF block phase. These results suggest that superconductivity and metallic phase are related to the insulating $\sqrt{5} \times \sqrt{5}$ block AF insulating phase. If the SC phase in $Rb_{0.82}Fe_{1.68}Se_2$ mesoscopically coexists with the block AF phase,[36–43] a striped phase may form on the interface region of the block AF phase and the SC phase due to the interaction between local moments and itinerant electrons. The latter can be viewed as dopants to a Mott insulator phase and naturally result in a stripe phase as in the case of copper oxides.[34] Since neutron is a bulk probe, we cannot conclusively determine whether the phase from which the $(\pi,0)$ spin excitations arise is superconducting or not.

In summary, we have discovered that the SC $Rb_{0.82}Fe_{1.68}Se_2$ has spin excitations near the $(\pi,0)$ wave vector that is disallowed in the Fermi surface nesting picture. Although such excitations do not appear to be directly coupled to superconductivity, its intensity gain in the SC sample is at the expense of spin-wave intensity reduction of the insulating phase. These results suggest the presence of local moments in the SC $Rb_{0.82}Fe_{1.68}Se_2$. In addition, the $(\pi,0)$ spin excitations in the SC $A_yFe_{1.6+x}Se_2$ are coupled to spin waves from the block AF phase in the same sample.

ACKNOWLEDGMENTS

We thank Qimiao Si and Leland Harriger for helpful discussions, M. B. Stone for ARCS experiments, and R. Zhang for sample growth at IOP. The work at UTK is supported by the US NSF-DMR-1063866 and NSF-OISE-0968226. Work at IOP is supported by the MOST of China 973 program (Grant No. 2012CB821400) and by NSFC-51002180. ORNL neutron scattering facilities are supported by the U.S. DOE, Division of Scientific User Facilities.

*pdai@utk.edu

[1] P. A. Lee, N. Nagaosa, and X. G. Wen, Rev. Mod. Phys. **78**, 17 (2006).
[2] R. Coldea, S. M. Hayden, G. Aeppli, T. G. Perring, C. D. Frost, T. E. Mason, S.-W. Cheong, and Z. Fisk, Phys. Rev. Lett. **86**, 5377 (2001).
[3] M. Fujita, H. Hiraka, M. Matsuda, M. Matsuura, J. M. Tranquada, S. Wakimoto, G. Y. Xu, and K. Yamada, J. Phys. Soc. Jpn. **81**, 011007 (2012).
[4] D. C. Johnston, Adv. Phys. **59**, 803 (2010).
[5] I. I. Mazin, Nature (London) **464**, 183 (2010).
[6] C. de la Cruz, Q. Huang, J. W. Lynn, J. Li, W. Ratcliff II, J. L. Zarestky, H. A. Mook, G. F. Chen, J. L. Luo, N. L. Wang, and P. Dai, Nature (London) **453**, 899 (2008).
[7] M. D. Lumsden, A. D. Christianson, D. Parshall, M. B. Stone, S. E. Nagler, G. J. MacDougall, H. A. Mook, K. Lokshin, T. Egami, D. L. Abernathy, E. A. Goremychkin, R. Osborn, M. A. McGuire, A. S. Sefat, R. Jin, B. C. Sales, and D. Mandrus, Phys. Rev. Lett. **102**, 107005 (2009).
[8] S. Chi, A. Schneidewind, J. Zhao, L. W. Harriger, L. Li, Y. Luo, G. Cao, Zhuan Xu, M. Loewenhaupt, J. Hu, and P. Dai, Phys. Rev. Lett. **102**, 107006 (2009).
[9] D. S. Inosov, J. T. Park, P. Bourges, D. L. Sun, Y. Sidis, A. Schneidewind, K. Hradil, D. Haug, C. T. Lin, B. Keimer, and V. Hinkov, Nat. Phys. **6**, 178 (2010).
[10] C. L. Zhang, M. Wang, H. Q. Luo, M. Y. Wang, M. S. Liu, J. Zhao, D. L. Abernathy, T. A. Maier, K. Marty, M. D. Lumsden, S. Chi, S. Chang, J. A. Rodriguez-Rivera, J. W. Lynn, T. Xiang, J. P. Hu, and Pengcheng Dai, Sci. Rep. **1**, 115 (2011).
[11] T. A. Maier and D. J. Scalapino, Phys. Rev. B **78**, 020514(R) (2008).
[12] M. M. Korshunov and I. Eremin, Phys. Rev. B **78**, 140509(R) (2008).
[13] J. G. Guo, S. F. Jin, G. Wang, S. C. Wang, K. X. Zhu, T. T. Zhou, M. He, and X. L. Chen, Phys. Rev. B **82**, 180520(R) (2010).
[14] A. Krzton-Maziopa, Z. Shermadini, E. Pomjakushina, V. Pomjakushin, M. Bendele, A. Amato, R. Khasanov, H. Luetkens, and K. Conder, J. Phys.: Condens. Matter **23**, 052203 (2011).
[15] M. H. Fang, H. D. Wang, C. H. Dong, Z. J. Li, C. M. Feng, J. Chen, and H. Q. Yuan, Europhys. Lett. **93**, 47004 (2011).
[16] A. F. Wang, J. J. Ying, Y. J. Yan, R. H. Liu, X. G. Luo, Z. Y. Li, X. F. Wang, M. Zhang, G. J. Ye, P. Cheng, Z. J. Xiang, and X. H. Chen, Phys. Rev. B **83**, 060512 (2011).
[17] L. Häggström, A. Seidel, and R. Berger, J. Magn. Magn. Mater. **98**, 37 (1991).
[18] W. Bao, Q. Huang, G. F. Chen, M. A. Green, D. M. Wang, J. B. He, X. Q. Wang, and Y. Qiu, Chin. Phys. Lett. **28**, 086104 (2011).
[19] V. Yu. Pomjakushin, D. V. Sheptyakov, E. V. Pomjakushina, A. Krzton-Maziopa, K. Conder, D. Chernyshov, V. Svitlyk, and Z. Shermadini, Phys. Rev. B **83**, 144410 (2011).
[20] F. Ye, S. Chi, Wei Bao, X. F. Wang, J. J. Ying, X. H. Chen, H. D. Wang, C. H. Dong, and Minghu Fang, Phys. Rev. Lett. **107**, 137003 (2011).
[21] Meng Wang, Miaoyin Wang, G. N. Li, Q. Huang, C. H. Li, G. T. Tan, C. L. Zhang, Huibo Cao, Wei Tian, Yang Zhao, Y. C. Chen, X. Y. Lu, Bin Sheng, H. Q. Luo, S. L. Li, M. H. Fang, J. L. Zarestky, W. Ratcliff, M. D. Lumsden, J. W. Lynn, and Pengcheng Dai, Phys. Rev. B **84**, 094504 (2011).

[22] Y. Zhang, L. X. Yang, M. Xu, Z. R. Ye, F. Chen, C. He, J. Jiang, B. P. Xie, J. J. Ying, X. F. Wang, X. H. Chen, J. P. Hu, and D. L. Feng, Nature Materials **10**, 273 (2011).

[23] T. Qian, X.-P. Wang, W.-C. Jin, P. Zhang, P. Richard, G. Xu, X. Dai, Z. Fang, J.-G. Guo, X.-L. Chen, and H. Ding, Phys. Rev. Lett. **106**, 187001 (2011).

[24] Daixiang Mou, Shanyu Liu, Xiaowen Jia, Junfeng He, Yingying Peng, Lin Zhao, Li Yu, Guodong Liu, Shaolong He, Xiaoli Dong, Jun Zhang, Hangdong Wang, Chiheng Dong, Minghu Fang, Xiaoyang Wang, Qinjun Peng, Zhimin Wang, Shenjin Zhang, Feng Yang, Zuyan Xu, Chuangtian Chen, and X. J. Zhou, Phys. Rev. Lett. **106**, 107001 (2011).

[25] I. I. Mazin, Physics **4**, 26 (2011).

[26] T. A. Maier, S. Graser, P. J. Hirschfeld, and D. J. Scalapino, Phys. Rev. B **83**, 100515(R) (2011).

[27] G. Friemel, J. T. Park, T. A. Maier, V. Tsurkan, Yuan Li, J. Deisenhofer, H.-A. Krug von Nidda, A. Loidl, A. Ivanov, B. Keimer, and D. S. Inosov, Phys. Rev. B **85**, 140511 (2012).

[28] J. T. Park, G. Friemel, Yuan Li, J.-H. Kim, V. Tsurkan, J. Deisenhofer, H.-A. Krug von Nidda, A. Loidl, A. Ivanov, B. Keimer, and D. S. Inosov, Phys. Rev. Lett. **107**, 177005 (2011).

[29] Miaoyin Wang, Chen Fang, Dao-Xin Yao, GuoTai Tan, Leland W. Harriger, Yu Song, Tucker Netherton, Chenglin Zhang, Meng Wang, Matthew B. Stone, Wei Tian, Jiangping Hu, and Pengcheng Dai, Nature Commun. **2**, 580 (2011).

[30] Q. Si and E. Abrahams, Phys. Rev. Lett. **101**, 76401 (2008).

[31] S. M. Hayden, H. A. Mook, P. Dai, T. G. Perring, and F. Doğan, Nature (London) **429**, 531 (2004).

[32] J. M. Tranquada, H. Woo, T. G. Perring, H. Goka, G. D. Gu, G. Xu, M. Fujita, and K. Yamada, Nature (London) **429**, 534 (2004).

[33] A. T. Boothroyd, P. Babkevich, D. Prabhakaran, and P. G. Freeman, Nature (London) **471**, 341 (2011).

[34] S. A. Kivelson, I. P. Bindloss, E. Fradkin, V. Oganesyan, J. M. Tranquada, A. Kapitulnik, and C. Howald, Rev. Mod. Phys. **75**, 1201 (2003).

[35] L. W. Harriger, H. Q. Luo, M. S. Liu, C. Frost, J. P. Hu, M. R. Norman, and P. Dai, Phys. Rev. B **84**, 054544 (2011).

[36] Y. J. Song, Z. Wang, Z. W. Wang, H. L. Shi, Z. Chen, H. F. Tian, G. F. Chen, H. X. Yang, and J. Q. Li, Europhys. Lett. **95**, 37007 (2011).

[37] A. Ricci, N. Poccia, G. Campi, B. Joseph, G. Arrighetti, L. Barba, M. Reynolds, M. Burghammer, H. Takeya, Y. Mizuguchi, Y. Takano, M. Colapietro, N. L. Saini, and A. Bianconi, Phys. Rev. B **84**, 060511 (2011).

[38] Z. Shermadini, H. Luetkens, R. Khasanov, A. Krzton-Maziopa, K. Conder, E. Pomjakushina, H-H. Klauss, A. Amato, Phys. Rev. B **85**, 100501(R) (2012).

[39] Wei Li, Hao Ding, Peng Deng, Kai Chang, Canli Song, Ke He, Lili Wang, Xucun Ma, Jiang-Ping Hu, Xi Chen, and Qi-Kun Xue, Nat. Phys. **8**, 126 (2012).

[40] F. Chen, M. Xu, Q. Q. Ge, Y. Zhang, Z. R. Ye, L. X. Yang, Juan Jiang, B. P. Xie, R. C. Che, M. Zhang, A. F. Wang, X. H. Chen, D. W. Shen, J. P. Hu, and D. L. Feng, Phys. Rev. X **1**, 021020 (2011).

[41] V. Ksenofontov, G. Wortmann, S. A. Medvedev, V. Tsurkan, J. Deisenhofer, A. Loidl, and C. Felser, Phys. Rev. B **84**, 180508(R) (2011).

[42] A. Charnukha, J. Deisenhofer, D. Pröpper, M. Schmidt, Z. Wang, Y. Goncharov, A. N. Yaresko, V. Tsurkan, B. Keimer, A. Loidl, and A. V. Boris, Phys. Rev. B **85**, 100504(R) (2012).

[43] C. C. Homes, Z. J. Xu, J. S. Wen, and G. D. Gu, Phys. Rev. B **85**, 180510(R) (2012).